Advanced Materials Research, 2010, Volumes 89 - 91, 615-620

MATERIAL CONSTITUTIVE BEHAVIOUR AND MICROSTRUCTURE STUDY ON ALUMINIUM ALLOYS FOR FRICTION STIR WELDING

H. Wang[1, a], P. Colegrove[1, b], H.M. Mayer[2], L. Campbell[3], R.D. Robson[3]

[1]Welding Engineering Research Centre, Cranfield University, Cranfield, MK43 0AL, UK

[2]Technische Universität Berlin, Berlin, Germany

[3]School of Material, University of Manchester, Manchester, M1 7HS, UK

[a]hua.wang@cranfield.ac.uk, [b]p.colegrove@cranfield.ac.uk

Keywords: Hot compression test; Al 6082 and 7449; High temperature and strain-rate; Subgrain; Friction stir welding model

Abstract. The material constitutive behaviour and microstructure of Aluminium alloys 6082 and 7449 were studied with the Gleeble hot compression test. The novel aspect of the work is that the testing was done at high strain-rates and at temperatures within 5 K of the solidus. The results indicated that the strength was maintained up to near solidus temperatures, with no dramatic strength reduction being observed. There was however, a distinct change in the slope observed with the 7449 results around 720 K. The experimental results were then fit to the Zener-Holloman equation, which describes the relationship between the material flow stress, temperature and strain-rates. The material microstructure of the hot compression test samples was analysed, and the averaged grain size was calculated to compare with friction stir weld nuggets. This will be used to infer the processing conditions that exist in the dynamically recrystallized weld nugget. Finally, a simple model was used to understand how processing conditions affected the deformation behaviour.

Introduction

A number of studies on hot workability have been accomplished to illustrate the material flow stress characterisation[1-3]. During hot working the material strain-hardens to a steady state value[4], and is balanced by recovery and dynamic recrystallization[5,6]. The Zener-Holloman equation is used to relate the flow stress to the deformation strain-rate and temperature[7]:

$$Z = \dot{\varepsilon} \exp(\frac{Q}{RT}) = A[\sinh(\alpha\sigma)]^n \quad (1)$$

where $\dot{\varepsilon}$ is the strain-rate, Q is the activation energy, R is the gas constant, T is the temperature, σ is the flow stress, and n, α and A are the material constants. The Zener-Holloman equation can be used to describe the material properties during friction stir welding (FSW), such as the model developed by Colegrove[8] on Aluminium alloy and Nandan et al.[9] on mild steel. However the material constants applied in these models are both from literature, which need further investigation, particularly for material near to the solidus temperature.

The objective of the present study is to predict a set of modified Zener-Holloman material constants for Aluminium alloys 6082T6 and 7449T7 with Gleeble experiments performed over a wide range of strain-rates and temperatures. The material constants are further investigated by being applied to a preliminary FSW model. Secondly some microstructural analysis has been carried out to assist the microstructural modelling work of FSW, and understand the subgrain size under the different deformation conditions.

Material and Experiments Description

The experiments were performed on Gleeble® 3800 machine at Technische Universität Berlin. The Gleeble machine is design as an integrated hydraulic servo system capable of 10 tons force in tension

or 20 tons force in compression with direct resistance heating system[10]. K type thermocouples were resistance welded to the sample to measure and control the sample temperature. To lubricate the sample surface in contact with the anvils, graphite foils were pasted with a nickel based anti-seize & lubricating compound. The specimens are cylindrical: 9.6 mm in diameter with a length of 15 mm for 6082, and 10 mm in diameter with a length of 15 mm for 7449. The chemical composition of the alloys is shown in Table 1. The 6082 samples were deformed at temperatures of 673, 723, 753, 773, 818 and 838 K (solidus 848 K), and at true stain-rates of approximately 1, 10, 50, 100 s^{-1}. The 7449 samples were deformed at temperatures of 673, 723, 753, and 768 K (solidus 773 K) at the same set of strain-rates as the 6082.

During the tests, the specimens were rapidly heated up to the desired temperature, and held for 30 seconds before being compressively deformed. They were air cooled five seconds after the deformation. The force and displacement data were recorded to calculate the true stress and strain. The barrelling of the samples was determined and was within a tolerable range.

	Cu	Mg	Si	Fe	Mn	Zn	Cr	Ti	Al
6082T6	0.04	0.74	0.87	0.28	0.51	0.01	<0.01	0.02	Bal.
7449T7	1.80	2.03	0.05	0.08	<0.01	8.36			Bal.

Table 1: Chemical composition (in wt.%) of Aluminium alloys 6082T6 and 7449T7

Experimental Results

Typical stress verses strain plots are shown in Fig. 1. The noise in the stress verses strain plots depended on the deformation conditions. As shown in Fig. 1, (a) and (b) which were acquired at two similar strain-rates but different temperatures, the plots exhibit more noise at higher temperatures. There is greater noise initially, which reduces as the test progresses. Fig. 1 (c) uses the same temperature as Fig. 1 (b) but a much higher strain-rate and has considerable amount of noise in the short duration test.

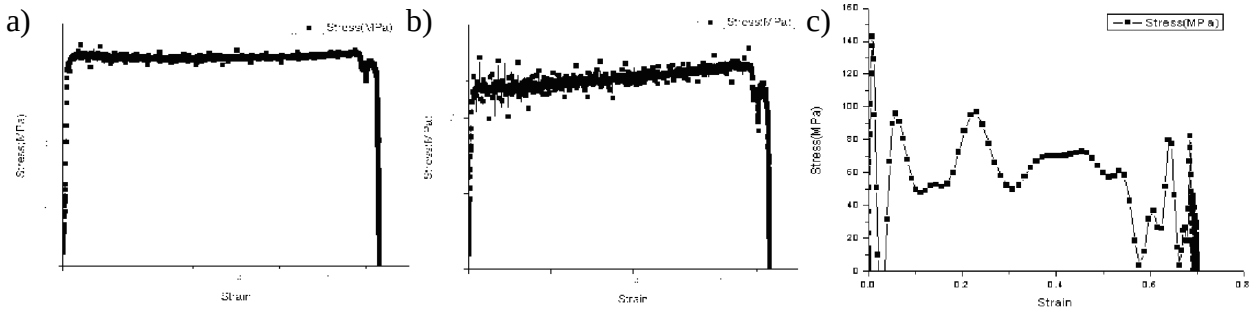

Fig. 1: Plots of stress vs. strain for Gleeble tests with deformation conditions at:
a) 673K, 0.932 s^{-1}; b) 818K, 0.945s^{-1}; c) 818K, 123.8s^{-1}

The deformation velocity of the machine was approximately constant which resulted in a varying strain-rate. Therefore average values of strain-rate and stress were calculated for each testing condition. The average stress is then plotted against the strain-rate, for the different temperatures used in the experiments (Fig. 2). A conventional curve fitting method is used to discover the Zener-Holloman material constants. Initially, different values of Q were selected within a reasonable range. For each value of Q the curves corresponding value of the Zener-Holloman parameter was found from:

$$Z = \dot{\varepsilon} \exp(Q/RT) \tag{2}$$

Afterwards, a commercial software package Origin was used to find material constants n, A and α (results shown in Table 2) using curve fitting with the following equation:

$$\sigma(Z) = \sinh^{-1}\left[(Z/A)^{\frac{1}{n}} \right] \Big/ \alpha \tag{3}$$

Values of R^2 were found for each value of Q. The value of Q that gave the highest value of R^2 was selected. The fitted curves including the experimental data are illustrated in Fig. 3. Note that there was

a distinct change in the slope around 720 K with the 7449 data, while no slope change was observed with the 6082 data. This characteristic is discussed in more depth later.

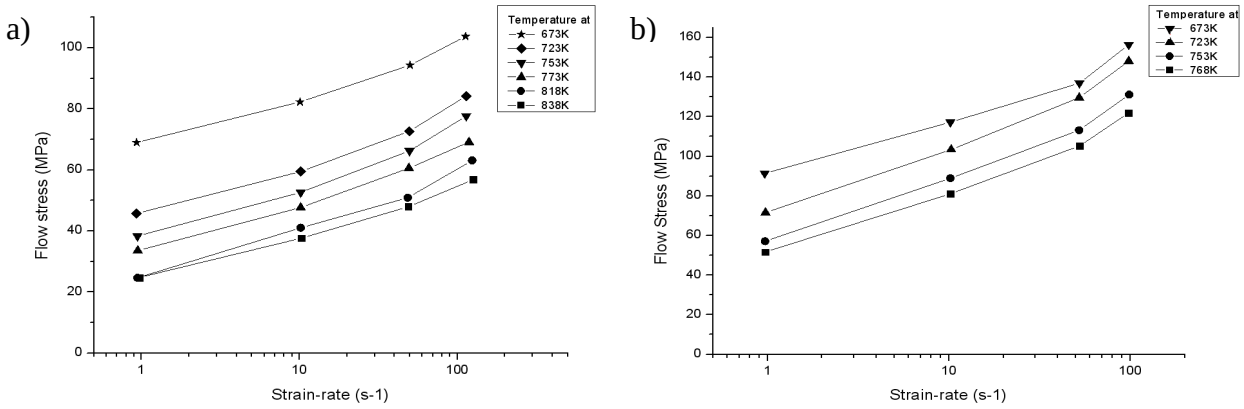

Fig. 2: The experimental measured stress values for a) 6082 and b) 7449, note that the strain-rate is in a logarithmic scale

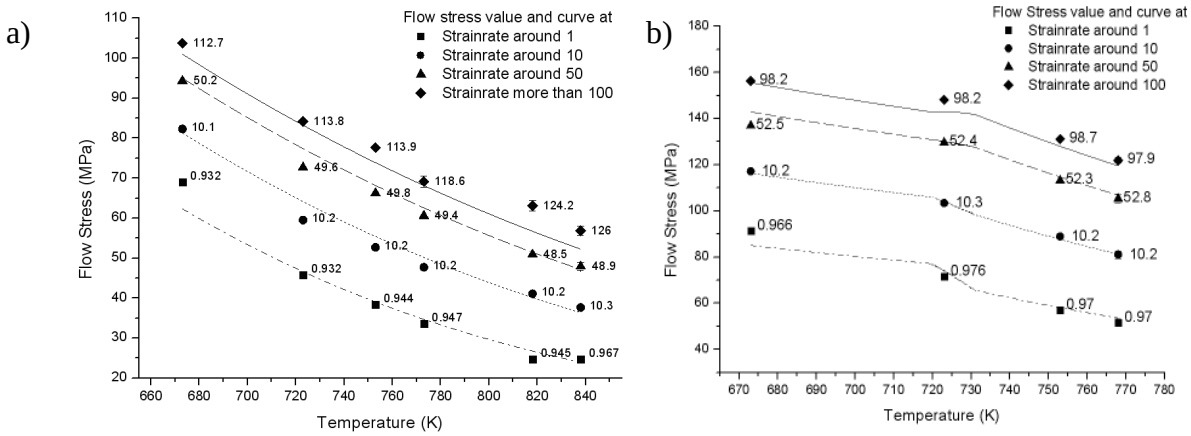

Fig. 3: Predicted material flow stress for a) 6082T6 and b) 7449T7 Aluminium alloys

Alloys	Q (J/mol)	A (s^{-1})	n	α (MPa^{-1})
6082T6	168000	3.0197E11	4.70929	0.02416
7449T7 at lower temperatures	60000	5.214E6	6.68309	0.00557
7449T7 at higher temperatures	140000	5.026E11	5.16663	0.00691

Table 2: Determined material constants for Aluminium alloys 6082T6 and 7449T7

Discussion

The novel aspect of the work is that the testing was done at high strain-rates (up to 120 s^{-1}) and near solidus temperature, which has not been previously investigated in the literature. The experimental material results for 6082 showed a reduction of flow stress with increasing the temperature, however no rapid softening regime occurred as temperature approached the solidus. The determined Zener-Holloman constants, such as the activation energy Q (16800 J/mol) suggests that the activation energy values described in the literatures[1,11] (143890, 153000 J/mol) were underestimated, which may possibly be due to the higher temperatures used in these tests. Under the same temperature and strain-rate condition, the Zener-Holloman equation with determined material constants predicts less flow stress compared to the literatures as the temperature approaching solidus.

The experimental results of 7449 showed an increase in slope when the temperature exceeded about 720 K. This slope change was greater at the higher strain-rates. A possible reason is that complete dissolution of the η and η' precipitates occurs about 723 K[12], which may lead to softening and the increase in slope above this temperature. For 7449 the discovered activation energy at higher temperatures (140000 J/mol) is much higher than one at lower temperatures (60000 J/mol), but only slightly higher than the one from the literature[1] (134158 J/mol). Under the same temperature and

strain-rate condition, the Zener-Holloman equation with determined material constants predicts at most 40% higher flow stress compared to the literatures, particularly at high strain-rate.
Although the noise increased with both temperature and strain-rate, the strain-rate had a greater influence. The higher noise at the start of the test is probably due to the initial impact load. There is an increase in stress over the duration of the test in Fig. 1 (b), but not the other conditions. The reason for this is uncertain. Finally the greater noise in the high temperature high strain-rate results may help explain the greater scatter observed in the high temperature and strain-rate in Fig. 3.

Microstructural analysis

Some microstructural analyses have been applied with Electron Backscatter Diffraction (EBSD) to study the subgrain sizes of the sample. The subgrain size are particularly important to prescribe the microstructural evolution during hot deformation, since it is highly relevant to most material mechanical properties[13], and the recrystallized grain size is also determined (before grain growth) by the subgrain size developed during deformation[14]. The results can be used for the validation of the microstructural models of FSW. The subgrain diameter d and Zener-Holloman parameter Z have the following relationship[15]

$$d^{-m} = a + b\ln(Z) \tag{4}$$

where m, a and b are material constants.
Analyzed samples conditions and results are shown in Table 3. The measured average subgrain sizes are similar to various microstructural model predicted curves, as shown in
Fig. 4. The optical Microscope (OM) results show much smaller sizes as they only focus on the unrecrystallized region. EBSD measured values distribute within the variations of the two different models.
All measured subgrain sizes are much smaller than ones of FSW nugget[16], and a comparison in Fig. 5 shows that the Gleeble sample is not typical of the FSW nugget, because the Gleeble sample graph shows a partially recrystallized microstructure while the FSW is uniform. It is because of the η precipitate particles at the grain/subgrain boundaries which prevent further boundary migration and therefore inhibit recrystallization. In addition, the strain in the Gleeble test is much lower and FSW material was deformed more uniformly.

Material	Temperature (K)	Strain-rate (s^{-1})	Subgrain sizes (micron)	Method
7449	753	94.4	5.77	EBSD
7449	768	52.5	4.66	EBSD
7449	768	94.3	3.71	OM
7449	768	96.3	3.27	OM

Table 3: Materials processed with microstructural analysis

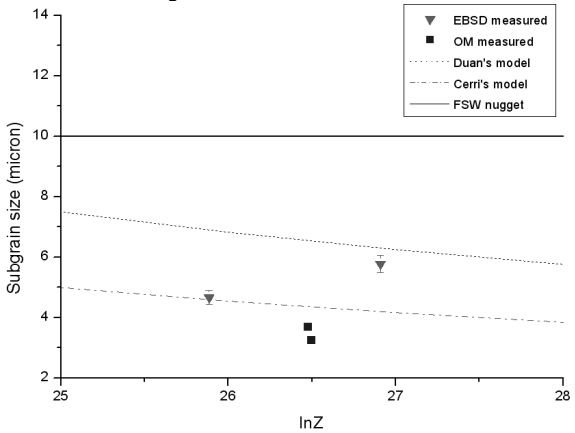

Fig. 4: Comparative plot of EBSD/OM measured subgrain sizes among simulated and SAXS measured FSW nugget results

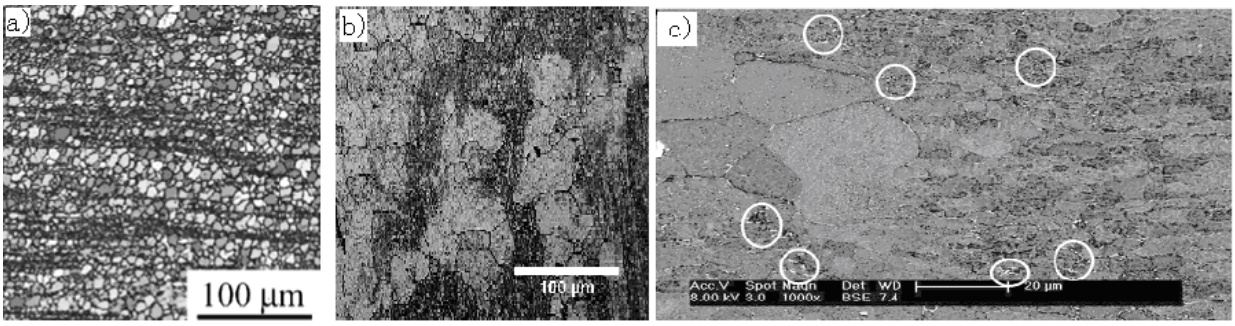

Fig. 5: Microstructure of AA7449, a) FSW nugget; b) Gleeble test, c) SEM micrograph of boundary precipitates for 7449 Gleeble sample, high angle boundary precipitates are circled

Application of the Zener-Holloman parameters

The Zener-Holloman equation with fitting parameters was applied to a preliminary high welding speed FSW model[8] of Aluminium alloy 6082T6, to understand how processing conditions affected the deformation behaviour. The weld plate was 350mm long, 220mm wide and 3.2mm thick. The welding tool had a shoulder with a radius of 7.5mm and a simple cylinder pin with a top radius of 2.5mm, bottom radius of 1.936mm and depth of 3.2mm. The other model settings such as the boundary conditions are the same as one developed by Colegrove[8]. The model was developed with CFD package, in which the heat generation term is the viscous dissipation within the deformed material. The material prescribed as fluid flow has a viscosity μ governed by:

$$\mu = \bar{\sigma}/3\dot{\bar{\varepsilon}} \tag{5}$$

where $\bar{\sigma}$ is the stress which is calculated from the Zener-Holloman equation, and $\dot{\bar{\varepsilon}}$ is the effective strain-rate. An empirical softening regime with a critical loss of flow strength from an arbitrarily defined softening temperature to the solidus temperature is assumed even though this was clearly not observed in the experiments. This approach has been used by Colegrove[8] and aids convergence.
Some streamline (Fig. 6(a)) plots were generated to investigate the material deformation condition under different welding parameters. A plot of strain-rate against temperature for different welding speeds (Fig. 6(b)) shows that the material was deformed at a lower strain-rate as the welding speed increased, and the material in front of pin was deformed at lower temperature as the welding speed increase.

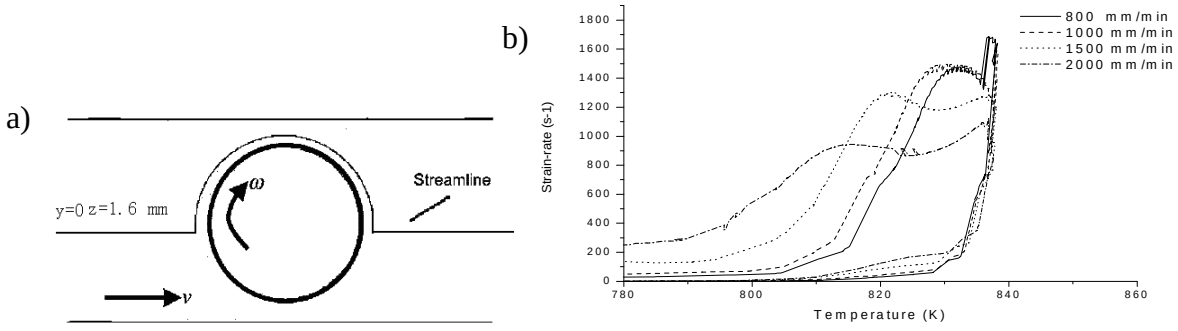

Fig. 6: a) A streamline travels around central of the weld pin; b) Comparison plot of predicted stress during welding using different welding speeds and a constant rotation speed of 2500RPM

Conclusions

1. No dramatic reduction in 6082 flow stress curve near the solidus temperature is observed.
2. Slight softening is observed in 7449 at temperatures above 720 K.
3. For 6082 a set of Zener-Holloman material constants were suggested. Two sets for 7449 of fitting parameters were found, one for the lower temperature where the slope is lower and one for the higher temperature where the slope is greater.

4. Noise increased with both temperature and strain-rate with strain-rate having the greater effect.
5. Influence of different welding speeds on material deformation was investigated by applying the new Zener-Holloman material constants on a FSW model.

Acknowledgements

The authors would like to acknowledge the financial support for this work by the Helmholtz Association through the Virtual Institute IPSUS, coordinated by GKSS Forschungszentrum Geesthacht, Germany.

References

[1] T. Sheppard, A. Jackson: *Constitutive equations for use in prediction of flow stress during extrusion of aluminium alloys*. Mater. Sci. and Tech. 13-3 (1997), p.203-209.

[2] H. Li, Z. Li, F. Guo, L. Meng, X. Liang: *Constitutive equation model for hot deformation of Al-Cu-Mg-Ag alloy*. Special Casting and Nonferrous Alloys. 28-11 (2008), p.823-826.

[3] Y-. Yi, J-. Yang, Y-. Lin: *Flow stress constitutive equation of 7050 aluminum alloy during hot compression*. Journal of Materials Engineering. 4-20 (2007), p.22-26.

[4] H.J. McQueen, N.D. Ryan: *Constitutive analysis in hot working*. Mater. Sci. and Eng. A. 322-1-2 (2002), p.43-63.

[5] H.J. McQueen, W.A. Wong, J.J. Jonas: *Discussion of dynamic recovery during hot working*. Acta Metallurgica 15-3 (1967), p.586-588.

[6] B. Verlinden, P. Wouters, H.J. McQueen, E. Aernoudt, L. Delaey, S. Cauwenberg: *Effect of different homogenization treatments on the hot workability of aluminium alloy AA2024*. Mater. Sci. and Eng. A. 123-2 (1990), p.229-37.

[7] C.M. Sellars, W.J.M. Tegart. *Hot workability*. Int. Met. Rev. 17 (1997), p.1-24.

[8] P.A. Colegrove, H.R. Shercliff, R. Zettler: *Model for predicting heat generation and temperature in friction stir welding from the material properties*. Sci. and Tech. of Wel. and Join. 12-4(2007), p.284-297.

[9] R. Nandan, G.G. Roy, T. J. Lienert, T. Debroy: *Three-dimensional heat and material flow during friction stir welding of mild steel*. Acta Materialia. 55-3(2007), p.883-895.

[10] Information available at: http://www.gleeble.com/3800.htm.

[11] X-. Li, J. Chen, H-. Zhang: Constitutive *model for hot deformation of 6082 aluminum alloy*. Chinese Journal of Nonferrous Metals. 18-10(2008), p.1769-74.

[12] N. Kamp, A. Sullivan, R. Tomasi, J.D. Robson: *Modelling of heterogeneous precipitate distribution evolution during friction stir welding process*. Acta Materialia. 54-8(2006), p.2003-14.

[13] X. Duan, T. Sheppard: *Influence of forming parameters on the final subgrain size during hot rolling of aluminium alloys*. Journal of Materials Processing Technology. 130-131(2002), p.245-9.

[14] F.J. Humphreys, M. Hatherly: Recrystallization and related annealing phenomena. Great British: Pergamon.1995.

[15] E. Cerri, E. Evangelista, A. Forcellese, H.J. McQueen. *Comparative hot workability of 7012 and 7075 alloys after different pretreatments*. Mater. Sci. and Eng. A. 197-2(1995), p.181-198.

[16] M. Dumont, A. Steuwer, A. Deschamps, M. Peel, P.J. Withers. *Microstructure mapping in friction stir welds of 7449 aluminium alloy using SAXS*. Acta Materialia. 54-18(2006), p.4793-4801.